Core-level photoemission studies of the α-Sn/InSb(100) heterostructure system

P. John, T. Miller, and T.-C. Chiang
Department of Physics, University of Illinois at Urbana-Champaign, 1110 West Green Street, Urbana, Illinois 61801 and Materials Research Laboratory, University of Illinois at Urbana-Champaign, 104 South Goodwin Avenue, Urbana, Illinois 61801
(Received 15 August 1988)

Layers of gray tin (α-Sn) were grown epitaxially on InSb(100) substrates at room temperature. The two high-quality InSb(100) reconstructions, Sb-stabilized $c(4\times4)$ and In-stabilized $c(8\times2)$, were used for starting surfaces. Core-level photoemission and electron diffraction were used to study the development of the interface as a function of Sn coverage and to determine the discontinuity in the valence-band maximum. For both starting surfaces, there was evidence for some Sb segregation into the Sn films during the initial stages of interface formation; the $c(4\times4)$ surface showed an earlier onset for the segregation. The Sn growth was found to be fairly flat for the first two layers, and three dimensional after that. The final valence-band discontinuity was found to be the same for both the $c(4\times4)$ and the $c(8\times2)$ starting surfaces. This discontinuity was compared to present theoretical predictions.

I. INTRODUCTION

Using the techniques of molecular-beam epitaxy (MBE), metastable films of gray tin (α-Sn) have been successfully grown on the high-symmetry faces of the lattice-matched compound semiconductors, InSb and CdTe.[1-6] The development and understanding of these types of custom-tailored heterostructures is important in generating new types of novel devices.[7-9] One of the key properties of a heterostructure device is the band offsets. Synchrotron photoemission can be used both to measure the valence-band offset and to gain insights into interfacial properties. This study will deal with the α-Sn/InSb(100) interface.

Previous high-energy electron diffraction (HEED) studies have shown that the InSb(100) surface exhibits two high-quality reconstructions: an In-stabilized $c(8\times2)$ structure, and a Sb-stabilized $c(4\times4)$ structure.[4,10-12] From core-level photoemission measurements, it has been determined that the $c(8\times2)$ surface is terminated by $\frac{3}{4}$ monolayer (ML) of In, while the $c(4\times4)$ surface is terminated by $1-\frac{3}{4}$ ML of Sb.[10] Based on these results and a comparison with the structural models for similarly reconstructed GaAs(100) surfaces, the surface structures of the InSb(100)-$c(8\times2)$ and -$c(4\times4)$ have been proposed to consist of $\frac{3}{4}$ ML of In and Sb dimers, respectively, on a monolayer-Sb-terminated surface. It is of great interest to examine whether or not the different surface reconstructions and compostional stoichiometries will have an effect on the band offsets when Sn is deposited on these surfaces to form a heterojunction.

In the present study, these surface structures, as well as Sn overlayers on these surfaces, were generated *in situ* via MBE. Previous studies have shown that accurate direct measurements of the energy of the valence-band maximum (VBM) relative to the Fermi level in a semiconductor can be made from photoemission spectra of the valence-band region, provided that surface state emission in the gap is negligible. If the substrate and overlayer valence-band features can be separately identified, then the band offset can be directly deduced from such measurements.[13,14] For the systems studied here, this method did not work well due to the ambiguity in distinguishing substrate emission from overlayer emission. For this reason a different scheme for determining the energy of the substrate VBM as a function of Sn coverage was employed.[14,15] The binding energies of the In 4*d* and Sb 4*d* core levels were measured with respect to VBM for the two clean surfaces. The binding energies of the bulk core levels were then used to track the relative energy position of the substrate VBM as Sn coverage was increased. Since core-level binding energies are generally affected by local bonding environments in addition to the band bending, it is important to distinguish the bulk core-level components from the surface-shifted components as well as any chemically shifted components which might be present near the interface.[14]

II. EXPERIMENTAL DETAILS

Photoemission experiments were conducted at the Synchroton Radiation Center of the University of Wisconsin–Madison, using the 1-GeV storage ring Aladdin. The University of Illinois "extended-range grasshopper" monochromator was used to disperse the light from the storage ring. An angle-integrated detection geometry was utilized for all photoemission spectra. All MBE was conducted in the photoemission chamber using a quartz-crystal thickness monitor to calibrate evaporation rates of the effusion cells. InSb substrate materials were obtained from Metal Specialities Inc. (Fairfield, Connecticut). Samples were oriented 3° off of the [100] direction toward the [011] direction to facilitate MBE growth, and then polished in this orientation with a solution of 0.05% bromine in methanol. A discussion of the

MBE generation techniques used for the InSb(100)-$c(4\times4)$ and InSb(100)-$c(8\times2)$ surfaces can be found elsewhere.[10] The Sn overlayers were prepared with the substrate at room temperature. The surface reconstructions were examined *in situ* with HEED.

III. RESULTS AND DISCUSSION

A. HEED and overlayer growth

HEED studies of the development of the Sn films grown on the two reconstructed InSb(100) surfaces indicated that both the $c(8\times2)$ and $c(4\times4)$ reconstructions are obliterated by the time the Sn coverage reaches 1 ML. For this study, 1 ML of Sn is defined to be the number of Sn atoms present in a single atomic (100) layer in the diamond structure of α-Sn, 4.76×10^{14} atoms/cm^2, which is the same as the atomic areal density for 1 ML of In or Sb in InSb. For the $c(4\times4)$ surface, the structure becomes predominantly (1×1) after 1 ML of Sn deposition, with some features of a (1×2) structure slightly visible. The background is also higher than that observed for the clean surface, indicating the presence of disorder. There is little change in the HEED pattern as the Sn coverage is increased to 2 ML; the only difference is that the slight (1×2) structure changes to a slight (2×1) structure. The alternation between one-domain (1×2) and (2×1) structure shows that the growth is nearly layer by layer; the stacking sequence of the substrate is felt by the surface, despite the disorder. This disorder is likely induced by the segregation of Sb in the Sn film as evidenced by core-level studies to be discussed below. Increasing the Sn coverage results in a very dim, high-background (1×1) structure that is maintained through 20 ML of Sn coverage. The HEED patterns in this coverage range suggest that the growth this three dimensional, perhaps induced by the initial disorder. The quality of the HEED pattern becomes much higher as the Sn coverage is increased to 100 ML. The pattern at 100 ML coverage indicates a very flat surface and the presence of mixed domains of (1×2) and (2×1) structures like that observed for the Ge and Si(100) surfaces, in agreement with the results of Hernández-Calderón and Höchst.[4] Thus, it appears that the initial disorder becomes outgrown at this coverage.

HEED shows that the development of the Sn film on the InSb(100)-$c(8\times2)$ surface is, in many respects, similar to that just discussed for the InSb(100)-$c(4\times4)$ surface. Yet there are some differences. For the $c(8\times2)$ surface no indication of (1×2) or (2×1) structures was observed until the high coverages ($\sim$100 ML) were achieved. For coverages less than 1 ML, faint streaks were present in the HEED pattern that were incommensurate with the substrate periodicity. This may indicate that there is a small amount of Sn in a β-Sn arrangement for these initial coverages.

B. Core-level photoemission intensity measurements

Low-resolution photoemission spectra of the 4*d* core levels of Sb, Sn, and In for both the $c(4\times4)$ and $c(8\times2)$ surfaces were recorded for the purpose of intensity measurements. A photon energy of 90 eV was utilized. Figure 1 shows the 4*d* core-level intensities as a function of Sn overlayer coverage on the InSb(100)-$c(4\times4)$ surface. The solid curves are the result of a layer attenuation calculation and represent the behavior of the three core-level intensities that would be expected for layer-by-layer growth of the Sn films on an abrupt interface. An electron escape depth of 6 Å is assumed.[10,16–18] As Fig. 1 indicates, the In and Sn core-level results agree with the layer-by-layer growth model for coverages up to about 2 ML. Beyond this coverage, the deviation becomes quite obvious; this is consistent with the HEED observation that the overlayer growth is three dimensional. The Sb core-level results deviate from the layer-by-layer model for coverages larger than about 0.5 ML. This behavior is explained by the segregation of Sb into the Sn film to be discussed in detail below. The segregation would cause the Sb intensity decay to be slower than that of the In.

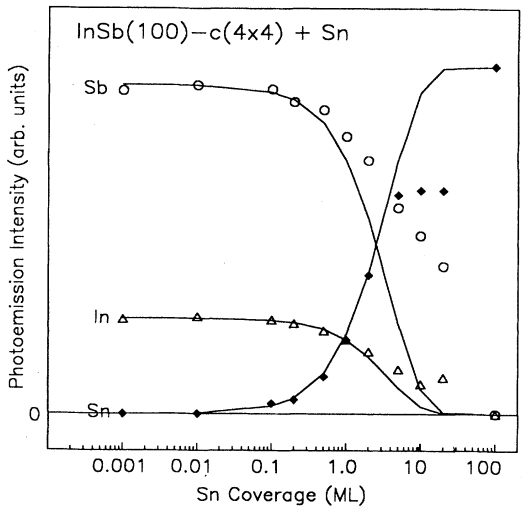

FIG. 1. Photoemission intensities for the Sb, In, and Sn 4*d* core levels plotted on a linear scale as a function of Sn coverage on the InSb(100)-$c(4\times4)$ surface. Measurements were made using a photon energy of 90 eV. The lines represent the behavior of the intensities that would be expected for layer-by-layer Sn growth on an abrupt interface.

Figure 2 shows the intensity results for Sn deposited on the InSb(100)-$c(8\times2)$ surface. As in Fig. 1, the solid curves in Fig. 2 represent the expected behavior for layer-by-layer growth on an abrupt interface. The solid curves describe the intensities for all three core levels very well for coverages up to 2 ML, and fails for coverages beyond 2 ML. Again, this is consistent with the HEED observations of three-dimensional growth. Three-dimensional Sn growth on the (110) face of InSb has also been observed.[5] The slower attenuation of the Sb intensity for the $c(4\times4)$ case in the coverage range of 1–2 ML can be related to the fact that the $c(4\times4)$ surface is much more Sb rich; thus, it is easier for Sb to segregate in the Sn overlayer.

Additional evidence for Sb segregation is presented in Fig. 3 which shows the ratios between the In 4*d* and Sb

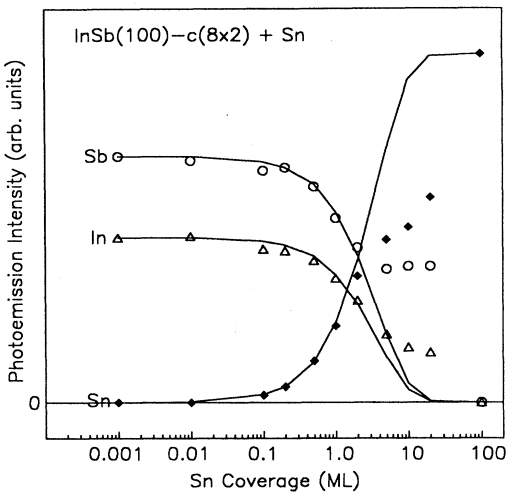

FIG. 2. Photoemission intensities for the Sb, In, and Sn 4*d* core levels plotted on a linear scale as a function of Sn coverage on the InSb(100)-$c(8\times2)$ surface. Measurements were made using a photon energy of 90 eV. The lines represent the behavior of the intensities that would be expected for layer-by-layer Sn growth on an abrupt interface.

4*d* core-level intensities for Sn coverages on both the $c(4\times4)$ and $c(8\times2)$ surfaces. For an abrupt interface, this ratio should remain constant. The decrease in this ratio is evidence of Sb diffusion into the Sn overlayers. The decrease becomes noticeable for Sn coverages above about 2 ML for the $c(8\times2)$ surface. For the $c(4\times4)$ surface, the ratio begins to decrease at approximately $\frac{1}{2}$ ML. Again, similar behavior has been reported for Sn on the InSb(110) surface.[5]

In both Figs. 1 and 2, the In and Sb core-level intensities become less than our detection limit (equivalent to 0.001 ML) at 100 ML Sn coverage. Thus, the Sb segregated into the Sn film becomes fully covered up and no pin holes are present in the Sn film at this coverage.

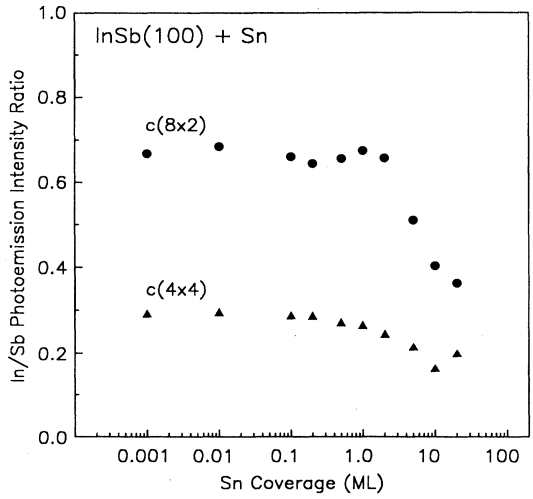

FIG. 3. Photoemission intensity ratios between the In and Sb 4*d* core levels as a function of Sn coverage on both the InSb(100)-$c(4\times4)$ and InSb(100)-$c(8\times2)$ surfaces.

C. Valence-band photoemission

Figure 4 shows the angle-integrated photoemission spectra of the VBM regions for the $c(4\times4)$ and $c(8\times2)$ surfaces. The binding energy is referenced to the Fermi level as measured from a gold foil in electric contact with the sample. If there is no occupied surface state within the gap contributing to the photoemission intensity, the spectra should reflect the bulk density of states broadened by the instrumental resolution. The theoretical bulk density of states near the VBM can be well approximated by an inclined straight line crossing the base line at the VBM. Thus, we extrapolate the upper edges of the spectra in Fig. 4 to the base lines as indicated, and obtain values of 0.45 and 0.32 eV below the Fermi level for the photoemission onset positions for the $c(4\times4)$ surface and $c(8\times2)$ surface, respectively. If this straight-line model function is convolved with the instrumental resolution function (well approximated by a Gaussian with a full width at half maximum of about 0.3 eV), only the portion near the onset is appreciably affected, and the result reproduces well the tailing of the spectra near the onset. Therefore, the onset positions determined here should be fairly accurate. We estimate the error to be no larger than 0.04 eV. The position of the onset should be the VBM, if there is no occupied surface state within the gap contributing to the photoemission intensity. Otherwise,

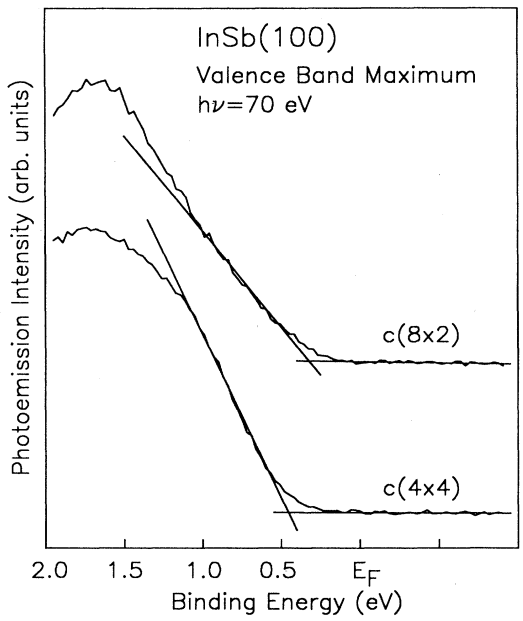

FIG. 4. Angle-integrated photoemission spectra near the VBM for both the InSb(100)–$c(4\times4)$ (bottom) and InSb(100)-$c(8\times2)$ (top) surfaces. Binding energies are referenced to the Fermi level E_F. The lines shown are extrapolations of the leading edges to determine the onset positions.

the VBM would be at a higher binding energy than that of the onset.

The energy-band gap for InSb is 0.18 eV; clearly the Fermi level is significantly above the conduction-band minimum for both of these surfaces. Because of the low conduction-band effective mass and very small band gap for InSb, a rather small doping level (10^{14} cm^{-3}) is sufficient to satisfy the Mott criterion for the onset of metallic behavior.[19,20] This doping level is most likely far exceeded in these samples by the very nature of the sample-preparation process. The density of states in InSb is quite small from the conduction-band minimum at Γ (0.18 eV above the VBM) up to the indirect minimum (0.62 eV above the VBM), so it is not surprising that the Fermi level lies within this range.[21] Very similar metallic behavior in InSb has also been observed in photoemission data recorded for the (110) face.[6]

A further comparison of the photoemission spectra of the valence-band regions for the two surfaces is given in Fig. 5. Here, the binding energies are referenced to the respective photoemission onset positions as determined from Fig. 4. Clearly, the valence-band features labeled in Fig. 5 are not aligned. Thus the onset positions do not reflect the VBM positions for one or both of the surfaces. This discrepancy is also evident in the difference in Sb 4*d* core-level binding energies for the $c(8\times2)$ and $c(4\times4)$ surfaces when they are referenced to the onset positions. Therefore, there must be a surface derived feature at or above the VBM for either or both of the two surfaces.

D. Valence-band maximum determined from the core-level energies

Figures 6 and 7 show the photoemission spectra for the Sb 4*d* and In 4*d* core levels, respectively, for the $c(4\times4)$ and $c(8\times2)$ surfaces. The dots represent the recorded data points and the curves through the dots are the results of fitting the data to Voigt line shapes. The binding-energy scales are referred to the Fermi level. For the spectrum which exhibited a resolved surface-shifted component, the fit is broken down into surface and bulk components and these components are shown directly beneath the data. The detailed analysis and interpretation of these core-level line shapes can be found elsewhere.[10] Briefly, the Sb-stabilized $c(4\times4)$ surface does not exhibit a surface shift for the In 4*d* core; the surface-shifted component for the Sb 4*d* core shown in Fig. 6 is the product of the three-fold-coordinated Sb atoms on the surface. The In-stabilized $c(8\times2)$ surface does not exhibit a surface shift for the Sb 4*d* core; the In 4*d* core does show a surface shift as evidenced by the broader line shape seen in Fig. 7. But the surface component is too close to the bulk component to be reliably resolved by the fitting procedure; no deconvolution of this spectrum is shown for this reason.

The position of the VBM is tied to the bulk core-level component independent of the band bending. From Fig. 6, the binding energies (with respect to the Fermi level) of

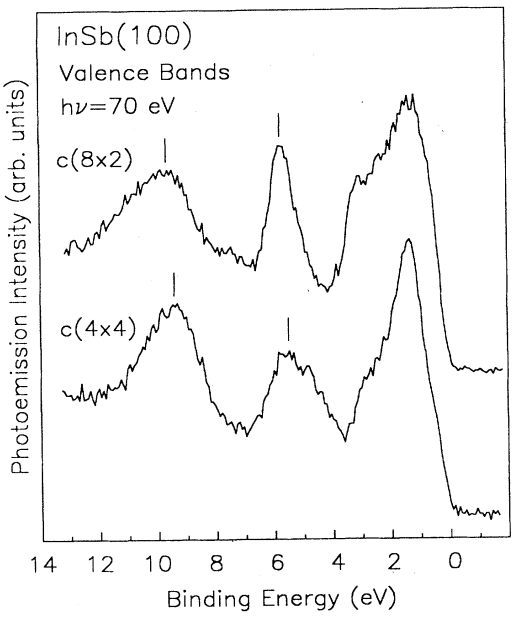

FIG. 5. Angle-integrated photoemission spectra of the valence region for both the InSb(100)-$c(4\times4)$ (bottom) and InSb(100)-$c(8\times2)$ (top) surfaces. Binding energies are referenced to the photoemission onset as measured from Fig. 4. The vertical dashes indicate features in the two spectra that are not aligned.

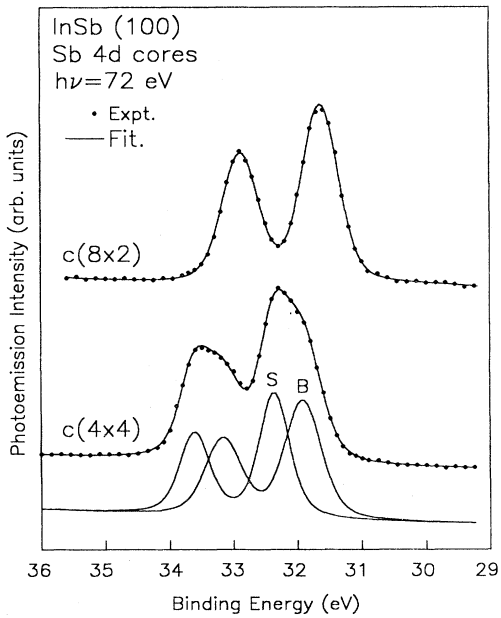

FIG. 6. Angle-integrated photoemission spectra of the Sb 4*d* core level for both the $c(4\times4)$ (bottom) and $c(8\times2)$ (top) surfaces. The dots represent data points, and the curves through the dots are fits to the data. For the $c(4\times4)$ spectrum, the surface (*S*) and bulk (*B*) components are displayed directly beneath the spectrum. No additional components were observed for the $c(8\times2)$ surface. Binding energies are referenced to the Fermi level.

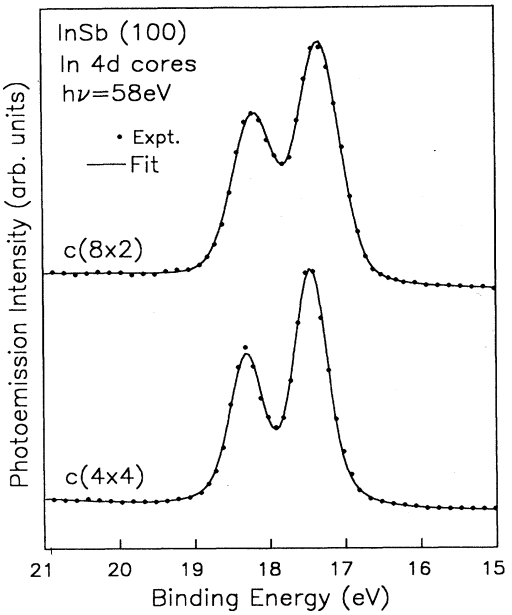

FIG. 7. Angle-integrated photoemission spectra of the In 4*d* core level for both the $c(4\times4)$ (bottom) and $c(8\times2)$ (top) surfaces. The dots represent data points, and the curves through the dots are single-component fits to the data. The $c(8\times2)$ spectrum shows a wider width, indicting the presence of unresolved surface shifts. Binding energies are referenced to the Fermi level.

the bulk components of the Sb $4d_{5/2}$ for the $c(4\times4)$ and $c(8\times2)$ are measured to be 31.92 and 31.63 eV, respectively. Denoting the binding energy of the VBM relative to the Fermi level by Δ, we then obtain the following relation:

$$\Delta[c(4\times4)]-\Delta[c(8\times2)]=0.29 \text{ eV} . \quad (1)$$

From earlier discussion of the photoemission onset position (see Fig. 4), we had

$$\Delta[c(4\times4)]\geq 0.45\pm0.04 \text{ eV} , \quad (2)$$

and

$$\Delta[c(8\times2)]\geq 0.32\pm0.04 \text{ eV} . \quad (3)$$

Furthermore, noting that the indirect conduction-band minimum represents the upper bound for the Fermi-level position for our nominally undoped samples, we obtain

$$\Delta[c(4\times4)]\leq 0.62 \text{ eV} . \quad (4)$$

Viewing Eqs. (1)–(4) as a whole places some tight constraints on the possible values of Δ. The allowed ranges of Δ are $\Delta[c(8\times2)]=0.28-0.33$ eV with 0.32 eV being the most probable value, and $\Delta[c(4\times4)]=0.57-0.62$ eV with 0.61 eV being the most probable value. For simplicity, we will use $\Delta[c(8\times2)]=0.32\pm0.04$ eV and $\Delta[c(4\times4)=0.61\pm0.04$ eV for the rest of the analysis. From Eqs. (2) and (3), it is clear that the onset of the spectrum for the $c(4\times4)$ surface in Fig. 4 is affected by surface-state emission. The onset of the spectrum for the $c(8\times2)$ surface represents the VBM within our experimental accuracy. The Fermi level of the $c(4\times4)$ surface is almost right at the indirect minimum of the conduction band.

E. Band offset determination

With increasing Sn coverages on these surfaces, the surface-shifted core-level components in all cases become diminished in intensity. After about 2 ML of Sn have been deposited on the surface, only the "bulk" core-level components remain visible. This single component, with a width generally somewhat larger than the width of the original bulk component, still consists of contributions from the atoms in the bulk, atoms at the interface, and any atoms that might have segregated into the Sn film. These separate contributions have essentially the same core-level binding energies within our experimental resolution; therefore, it becomes impossible or unnecessary to deconvolve the core-level line shapes. Figure 8 shows the surface-to-bulk intensity ratio for the Sb 4*d* core level for the $c(4\times4)$ surface as a function of Sn coverage. As can be observed, the surface-shifted component diminishes for increasing Sn coverages.

To estimate the effect and magnitude of the remaining small unresolved shifts after Sn coverage on the surface, we show in Fig. 9 the difference in binding energy between the bulk In and Sb $4d_{5/2}$ core levels as a function of Sn coverage for both the $c(4\times4)$ and $c(8\times2)$ surfaces. The differences should remain constant and equal for both surfaces provided there are no significant contributions from unresolved small shifts. In the case of $c(8\times2)$, the In 4*d* core level has an unresolved surface shift as discussed above (see Fig. 7); but the true bulk position cannot be determined by deconvolution, and therefore we simply used the overall peak position in this case.

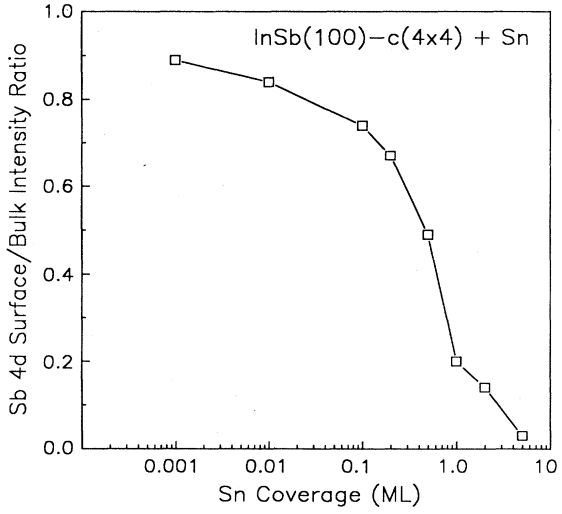

FIG. 8. Surface-to-bulk photoemission intensity ratio for the Sb 4*d* core level for the $c(4\times4)$ surface as a function of Sn coverage.

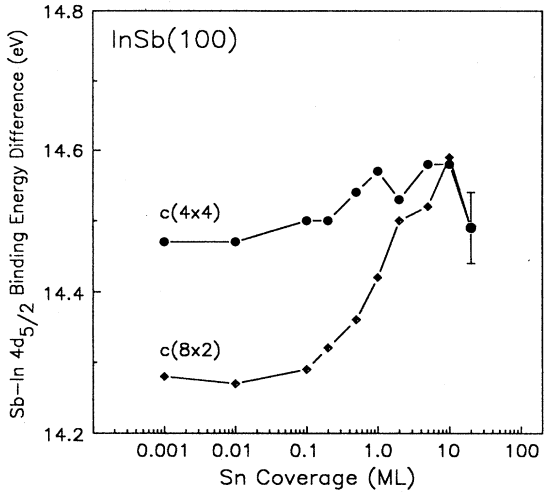

FIG. 9. Binding-energy difference between the bulk Sb $4d_{5/2}$ and In $4d_{5/2}$ core levels as a function of Sn coverage for both the $c(4\times4)$ and the $c(8\times2)$ surfaces.

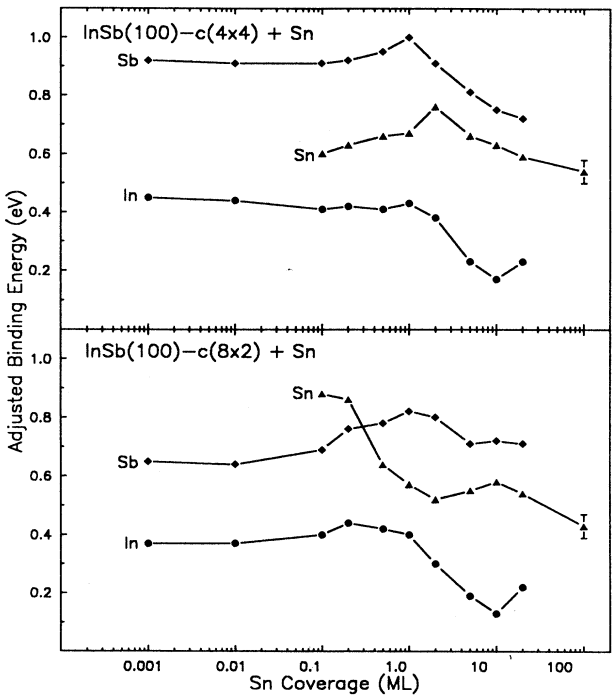

FIG. 10. Binding energies of the bulk Sb, In, and Sn $4d_{5/2}$ core levels as a function of Sn coverage. Binding energies for the $c(4\times4)$ surface are shown in the top panel; those for the $c(8\times2)$ surface are shown in the bottom panel. Binding energies shown are adjusted for a constant offset; to obtain the correct binding energies (as referenced to the Fermi level), add 31 eV to the Sb energies, 17 eV to the In energies, and 23.6 eV to the Sn energies.

Figure 9 shows that the binding-energy difference does not vary much for the $c(4\times4)$ surface. But a large variation is observed for the $c(8\times2)$ surface for Sn coverages below 2 ML due to the unresolved In $4d$ core surface shift just mentioned. This surface shift disappears beyond 2 ML coverage. The results in Fig. 9 show that at higher Sn coverages the uncertainties in the bulk core-level binding energies become small.

Figure 10 shows the binding energies of the bulk Sn, In, and Sb $4d$ core levels relative to the Fermi level as a function of Sn coverage for the $c(4\times4)$ and $c(8\times2)$ surfaces; for display purposes the energies have been offset by constant values given in the figure caption. Again, the data points for the In $4d$ core of the $c(8\times2)$ surface are affected by the unresolved surface shift for Sn coverages below 2 ML. The rest of the data should fairly accurately reflect the movement of the VBM relative to the Fermi level. The Sn $4d$ core-level energies are quite different at low coverages for these two surfaces; this difference may be a result of different amounts of Sb segregation and the different initial growth behaviors discussed above. The most important feature to note in Fig. 10 is the final energy positions of the Sn, In, and Sb core levels. From this the valence-band discontinuity for this heterojunction system can be deduced (the VBM for the α-Sn film is the Fermi level). The value for the valence-band discontinuity is determined to be 0.40 ± 0.06 eV, and is the same for both the $c(4\times4)$ and $c(8\times2)$ surfaces. The error of 0.06 eV represents the quadrature sum of the 0.04-eV error in the VBM position for the clean surfaces and the estimated 0.05-eV error in the final core-level binding energies. It is likely that the initial enhanced Sb segregation into the Sn for the Sb-rich $c(4\times4)$ surface produces similar chemical profile in the final heterojunctions formed on both the $c(4\times4)$ and $c(8\times2)$ surfaces, and hence the same discontinuity is obtained. For comparison, Förster, Tulke, and Lüth found the valence-band discontinuity to be 0.28 eV for Sn layers grown on the InSb(110) cleaved surface.[6]

Many attempts have been made to predict heterostructure band discontinuities through theoretical approaches.[22–25] One of the more successful methods is the semiempirical method developed by Tersoff.[21,26–29] The Tersoff model is based upon the concept that interface states in the gap are filled up to some midgap point. This midgap point is the point at which states change over from being primarily valencelike in character to being primarily conductionlike in character. When two semiconductors are brought together, these midgap points line up (with some corrections for the differences in electronegativity) and thereby determine the band discontinuities. For the α-Sn/InSb system, this model predicts a discontinuity in the VBM of 0.33 eV. Considering the uncertainty in this model (for example, no provision is made for the different crystallographic planes), this value is in fairly good agreement with the value of 0.40 ± 0.06 eV measured here.[6]

It should be noted that this model does not constrain the midgap point to fall within the actual band gap for the material. The Γ minimum at the zone center is ignored in this model, and the indirect gap is used in the calculation.[21] The reasoning behind this is that the in-

direct minima at the zone faces are more characteristic of the conduction bands than the Γ minimum. Furthermore, there is a very low density of states between the Γ minimum and the indirect minimum. This reasoning is supported by the observations here of the final Fermi-level position for both surfaces to be above the Γ minimum.[21]

Another model which has had some success in producing results consistent with experiment is the tight-binding approach developed by Harrison and Tersoff.[30,31] This method yields a valence-band offset of 0.61 eV for the α-Sn/InSb system. This number is considerably higher than the value of 0.40 eV measured here. The source of the discrepancy could be the failure to take spin-orbit splitting into effect. For the antimonides, corrections for spin-orbit splitting can be on the order of 0.3 eV.[31]

IV. SUMMARY

α-Sn growth on InSb(100)-$c(4\times4)$ and InSb(100)-$c(8\times2)$ has been characterized with core-level photoemission and high-energy electron diffraction. The initial growth of Sn up to about 2 ML was found to be relatively flat, and became three dimensional after that. For both surfaces, there was evidence for Sb segregation into the Sn films, and the degree of segregation was higher for the Sb-stabilized $c(4\times4)$ surface. For Sn coverages over about 100 ML, the overlayer became quite flat again, and exhibited a sharp two-domain (2×1) reconstruction characteristic of the α-Sn(100) surface. The discontinuity in the VBM was determined by tracking the binding energies of the bulk core-level components, and was measured to be 0.40±0.06 eV for both the $c(4\times4)$ and $c(8\times2)$ surfaces. These results are reconciled with current models for heterojunction band offsets.

ACKNOWLEDGMENTS

This material is based upon work supported by the U.S. Department of Energy (Division of Materials Sciences of the Office of Basic Energy Sciences) under Contract No. DE-AC02-76ER01198. Some of the personnel and equipment support was also derived from grants from the National Science Foundation (under Grants No. DMR-83-52083 and No. DMR-86-14234), the IBM Thomas J. Watson Research Center (Yorktown Heights, New York), and the E. I. du Pont de Nemours and Company (Wilmington, Delaware). The Synchrotron Radiation Center of the University of Wisconsin–Madison is supported by the National Science Foundation under Contract No. DMR-80-20164. We acknowledge the use of central facilities of the Materials Research Laboratory of the University of Illinois, which is supported by the U.S. Deparment of Energy (Division of Materials Sciences of the Office of Basic Energy Sciences), under Contract No. DE-AC02-76ER01198, and by the National Science Foundation under Contract No. DMR-86-12860.

[1]R. F. C. Farrow, D. S. Robertson, G. M. Williams, A. G. Cullis, G. R. Jones, I. M. Young, and P. N. J. Dennis, J. Cryst. Growth **54**, 507 (1981).
[2]S. Takatani and Y. W. Chung, Phys. Rev. B **31**, 2290 (1985).
[3]H. Höchst and I. Hernández-Calderón, Surf. Sci. **126**, 25 (1983); J. Vac. Sci. Technol. A **3**, 911 (1985); I. Hernández-Calderón and H. Höchst, Surf. Sci. **152**, 1035 (1983).
[4]I. Hernández-Calderón and H. Höchst, Phys. Rev. B **27**, 4961 (1983).
[5]M. Mattern and H. Lüth, Surf. Sci. **126**, 502 (1983).
[6]A. Förster, A. Tulke, and H. Lüth, J. Vac. Sci. Technol. B **5**, 1054 (1987).
[7]F. Capasso, Surf. Sci. **132**, 527 (1983).
[8]H. Kroemer, Surf. Sci. **132**, 543 (1983).
[9]H. C. Casey and M. B. Panish, *Heterostructure Lasers* (Academic, New York, 1978).
[10]P. John, T. Miller, and T.-C. Chiang, Phys. Rev. B **39**, 1730 (1989).
[11]K. Oe, S. Ando, and K. Sugiyama, Jpn. J. Appl. Phys. **19**, L47 (1980).
[12]A. J. Noreika, M. H. Francombe, and C. E. C. Wood, J. Appl. Phys. **52**, 7416 (1981).
[13]G. Margaritondo, Solid State Electron **26**, 499 (1983).
[14]T.-C. Chiang, CRC Crit. Rev. Solid State Mater. Sci. **14**, 269 (1988).
[15]J. R. Waldrop, R. W. Grant, and E. A. Kraut, J. Vac. Sci. Technol. B **4**, 1060 (1986).
[16]P. John, F. M. Leibsle, T. Miller, T. C. Hsieh, and T.-C. Chiang, Superlatt. Microstruct. **3**, 347 (1987).
[17]T.-C. Chiang, Comments At. Mol. Phys. **13**, 299 (1983).
[18]C. R. C. Brundle, J. Vac. Sci. Technol. **11**, 212 (1974).
[19]P. A. Cox, *The Electronic Structure and Chemistry of Solids* (Oxford Science, New York, 1987).
[20]J. Kolodziejczak, Acta Phys. Pol. **20**, 289 (1961).
[21]J. Tersoff, Phys. Rev. B **32**, 6968 (1985).
[22]W. R. Frensley and H. Kroemer, J. Vac. Sci. Technol. **13**, 810 (1976).
[23]J. L. Freeouf and J. M. Woodall, Appl. Phys. Lett. **39**, 727 (1981).
[24]C. Mailhiot and C. B. Duke, J. Vac. Sci. Technol. A **4**, 869 (1986).
[25]C. Tejedor and F. Flores, J. Phys. C **11**, L19 (1978).
[26]J. Tersoff, Phys. Rev. Lett. **52**, 465 (1984).
[27]J. Tersoff, Phys. Rev. B **30**, 4874 (1984).
[28]J. Tersoff, Phys. Rev. Lett. **56**, 675 (1986).
[29]J. Tersoff, Phys. Rev. Lett. **56**, 2755 (1986).
[30]W. A. Harrison, J. Vac. Sci. Technol. **14**, 1016 (1977).
[31]W. A. Harrison and J. Tersoff, J. Vac. Sci. Technol. B **4**, 1068 (1986).